

An experimental and theoretical study of the glass-forming region of the Mg–Cu–Sn system

J. A. SOMOZA, L. J. GALLEGO*, C. REY

Departamento de Física de la Materia Condensada, Facultad de Física, Universidad de Santiago de Compostela, Santiago de Compostela, Spain

S. ROZENBERG, B. ARCONDO, H. SIRKIN†

Departamento de Física, Facultad de Ingeniería, UBA, Paseo Colón 850, 1063 Buenos Aires, Argentina

R. H. DE TENDLER, J. A. KOVACS

Gerencia de Desarrollo, Comisión Nacional de Energía Atómica, Avda. del Libertador 8250, 1429 Buenos Aires, Argentina

J. A. ALONSO

Departamento de Física Teórica, Facultad de Ciencias, Universidad de Valladolid, Valladolid, Spain

The amorphization of Mg–Cu–Sn alloys with various compositions has been studied using the melt-spinning technique, with particular emphasis on the magnesium-rich corner of the ternary phase diagram. The results have been interpreted in terms of Miedema's theory, which highlights competition between the amorphous phase and crystalline solid solutions. Competition by ordered intermetallic compounds has also to be considered in order to explain the restricted amorphization region found in these experiments.

1. Introduction

In recent years, both thermodynamic and kinetic aspects of the glass-forming ability (GFA) of binary metal systems have been extensively discussed (see, for example, [1–3]). Factors usually accepted as affecting GFA in binary alloys include size mismatch, valence, electronegativity, composition and the enthalpy of formation of defects such as vacancies [4]. Most of these factors are explicitly used in a semiempirical approach developed by Miedema and co-workers [5, 6] and by some of the present authors [7–9]. This approach, which is capable of predicting the possible glass-forming concentration ranges of binary transition metal alloys, is basically a combination of classical elasticity theory [10] and Miedema's model for the heat of formation of alloys [11], and constitutes an alternative to other thermodynamic treatments of glass formation such as the CALPHAD method (see, for example, [12, 13]).

Theoretical studies of the GFA of alloys with more than two components are scarce. However, from the few carried out so far it has become clear that such factors as atomic size mismatch play a key role in determining the GFA of these systems too. For instance, Sommer *et al.* [14] have found that glass formation is possible in ternary magnesium-based alloys when the relative difference $|r_{\text{Mg}} - \bar{r}|/\bar{r}$, where

r_{Mg} is the atomic radius of magnesium and \bar{r} , the mean of the atomic radii of the other two components, is greater than 10%; Ueno and Waseda [15] have proposed an empirical equation for calculating the minimum solute concentration for glass formation in ternary alloys from the relative sizes of the components. Ueno and Waseda's equation is an extension of that proposed by Egami and Waseda [16] for binary alloys on the basis of an atomic elasticity theory.

In order to obtain a method for quantitative estimation of the glass-forming concentration regions of multicomponent alloys, we have extended Miedema's theory to the ternary case [17]. The extension is not trivial due to the problem of calculating the size mismatch effect in this kind of system. As an application of the theory, we studied the amorphization of the Cu–Ti–Zr system [17], whose glass-forming behaviour under melt-spinning shows the influence of competing crystal structures [18]. Further studies of other ternary alloys are evidently necessary. In the present work we explored the model by studying the ternary alloy Mg–Cu–Sn, checking the theoretical predictions against our own experimental data on the glass-forming region of this alloy, and against additional experimental information for the magnesium-rich corner of the Mg–Cu–Sn phase diagram [19, 20]. Sommer *et al.* [19] have carried out microcalorimetric measure-

* Author to whom all correspondence should be addressed.

† CONICET career research worker.

ments of relaxation phenomena in magnesium-rich Mg–Cu–Sn glasses, and Sirkin *et al.* [20] have used Mössbauer spectroscopy and X-ray diffraction to study how the addition of tin increases the glass-forming concentration range of rapidly quenched samples of Mg–Cu (and Mg–Zn) binary alloys. The binary amorphous system Mg–Cu has recently been studied theoretically by de Tandler *et al.* [9] on the basis of Miedema's theory, and our study can be considered as an extension of that work, mainly oriented towards investigating the influence of the addition of tin on the GFA of Mg–Cu.

Some details of the experimental procedure used are presented together with the results obtained. The theoretical model used to calculate the Gibbs free energies of mixing of the competing phases in ternary alloys with GFA is briefly described; a more detailed description can be found elsewhere [17]. The results of our calculations for the Mg–Cu–Sn system and their comparison with the experimental data are presented.

2. Experimental procedure and results

In order to determine the glass-forming composition range of the Mg–Cu–Sn system, experiments were performed on samples from various regions of the phase diagram (Table I). Some of the samples correspond to characteristic points studied in previous work [20–23]. The alloys labelled A1–A11 in Table I were prepared from 99.99% pure materials by melting under an argon atmosphere. Their homogeneity was checked by metallographic inspection. These alloys were quenched with a single-roller melt-spinning apparatus to obtain samples in ribbon form which had an average thickness of 20–40 μm and were analysed, as were the crystallization products of the same melts, by X-ray diffraction (XRD) with CuK_α radiation. The results for alloys labelled B1–B5 in Table I were obtained previously by some of us [20] with the same

equipment and under identical conditions as those for A1–A11. Some characteristics of the samples studied and the results of our XRD analyses are summarized below.

A1: $\text{Mg}_{94.52}\text{Cu}_{2.65}\text{Sn}_{2.83}$. According to Chang *et al.* [21], the products of the crystallization process are magnesium as a primary phase, the binary eutectic Mg– Mg_2Sn and the ternary eutectic Mg– Mg_2Cu – Mg_2Sn . These three phases were all observed by us using XRD. The rapidly quenched samples presented a crystalline XRD pattern in which magnesium and Mg_2Cu were identified; neither Mg_2Sn , nor tin in solid solution in magnesium or Mg_2Cu , were observed. Mg_2Sn may be present as a dispersed phase.

B1: $\text{Mg}_{88}\text{Cu}_2\text{Sn}_{10}$. The composition of this alloy is approximately located in the Mg– Mg_2Sn eutectic valley [22], in accordance with which the crystallization products are the Mg– Mg_2Sn eutectic plus the ternary Mg– Mg_2Cu – Mg_2Sn eutectic. Rapidly quenched samples are partially amorphous, crystalline magnesium and Mg_2Sn phases being identified as competing with glass formation [20].

B2: $\text{Mg}_{86}\text{Cu}_5\text{Sn}_9$. The products of the crystallization process are the same as those of sample B1 [22]. Rapidly quenched samples are partially amorphous, the crystalline phases competing with glass formation being magnesium and traces of the compound Mg_2Sn [20].

A2: $\text{Mg}_{85.45}\text{Cu}_{8.97}\text{Sn}_{5.58}$. The equilibrium structures are magnesium as primary phase, the binary eutectic Mg– Mg_2Sn and the ternary eutectic Mg– Mg_2Cu – Mg_2Sn [21]. Rapidly quenched samples were partially amorphous. Magnesium and traces of Mg_2Cu were observed competing with glass formation.

B3: $\text{Mg}_{85}\text{Cu}_9\text{Sn}_6$. Not far from the composition of A2, rapidly quenched samples become fully amorphous [20]. This composition may be considered as a limit for complete amorphization.

TABLE I XRD results for the samples studied. C, crystalline; PA, partially amorphous; T, traces (when small lines attributable to some crystalline phase are superimposed on the halo pattern); *, unknown equilibrium phases

Sample	Composition (at %)			Equilibrium phases	Fast-quenching results	
	Mg	Cu	Sn		Structure	Identified phases
A1	94.52	2.65	2.83	Mg, Mg_2Sn , Mg_2Cu	C	Mg, Mg_2Cu
B1	88.00	2.00	10.00	Mg, Mg_2Sn , Mg_2Cu	PA	Mg, Mg_2Sn
B2	86.00	5.00	9.00	Mg, Mg_2Sn , Mg_2Cu	PA	Mg, Mg_2Sn (T)
A2	85.45	8.97	5.58	Mg, Mg_2Sn , Mg_2Cu	PA	Mg, Mg_2Cu (T)
B3	85.00	9.00	6.00	Mg, Mg_2Sn , Mg_2Cu	A	
B4	82.00	6.00	12.00	Mg, Mg_2Sn , Mg_2Cu	PA	Mg_2Sn , Mg
A3	70.00	10.00	20.00	Mg, Mg_2Sn , Mg_2Cu	C	Mg_2Sn , Mg_2Cu
A4	78.37	12.00	9.63	Mg, Mg_2Sn , Mg_2Cu	A	
B5	76.00	18.00	6.00	Mg, Mg_2Sn , Mg_2Cu	A	
A5	74.24	22.72	3.04	Mg, Mg_2Sn , Mg_2Cu	A	
A6	82.68	12.32	5.00	Mg, Mg_2Sn , Mg_2Cu	A	
A7	63.60	28.07	8.33	Mg_2Sn , Cu_2Mg , Mg_2Cu	PA	Mg_2Sn (T), Mg_2Cu (T)
A8	61.20	19.40	19.40	Cu_2Mg + Sn in solution, Mg_2Sn , Mg_2Cu	C	Mg_2Sn
A9	52.00	24.10	23.90	Cu_2Mg + Sn in solution, Mg_2Sn ,*	C	Mg_2Sn , Cu_2Mg + Sn in solution
A10	33.33	33.33	33.33	MgCuSn ,*	C	MgCuSn
A11	16.66	66.67	16.66	Cu_4MgSn	C	Cu_4MgSn

B4: $\text{Mg}_{82}\text{Cu}_6\text{Sn}_{12}$. The products of the crystallization process are Mg_2Sn as primary phase plus the eutectics $\text{Mg}_2\text{Sn}-\text{Mg}$ and $\text{Mg}_2\text{Cu}-\text{Mg}-\text{Mg}_2\text{Sn}$ [21, 22]. Rapid quenching affords an amorphous phase and, in addition, crystalline Mg_2Sn and Mg phases [20].

A3: $\text{Mg}_{70}\text{Cu}_{10}\text{Sn}_{20}$. The equilibrium structure consists of Mg_2Sn as primary phase, the binary eutectic $\text{Mg}_2\text{Cu}-\text{Mg}_2\text{Sn}$ and the ternary eutectic $\text{Mg}_2\text{Cu}-\text{Mg}_2\text{Sn}-\text{Mg}$ [21, 22]. Only Mg_2Sn and Mg_2Cu were observed in the rapidly quenched samples.

A4: $\text{Mg}_{78.37}\text{Cu}_{12}\text{Sn}_{9.63}$; B5: $\text{Mg}_{76}\text{Cu}_{18}\text{Sn}_6$. The crystallization products are the same as those of alloy A3. Rapidly quenched samples were amorphous.

A5: $\text{Mg}_{74.24}\text{Cu}_{22.72}\text{Sn}_{3.04}$. The equilibrium structure consists of Mg_2Cu as primary phase, the binary eutectic $\text{Mg}_2\text{Cu}-\text{Mg}_2\text{Sn}$ and the ternary eutectic $\text{Mg}_2\text{Cu}-\text{Mg}_2\text{Sn}-\text{Mg}$ [21, 22]. The rapidly quenched samples were amorphous.

A6: $\text{Mg}_{82.68}\text{Cu}_{12.32}\text{Sn}_5$. Not far from the ternary eutectic composition $\text{Mg}_{82.10}\text{Cu}_{13.50}\text{Sn}_{4.40}$ [21, 22], the equilibrium phases Mg_2Sn , Mg_2Cu and magnesium were observed. Rapidly quenched samples were completely amorphous.

A7: $\text{Mg}_{63.60}\text{Cu}_{28.07}\text{Sn}_{8.33}$. This composition corresponds to that of the $\text{Mg}_2\text{Sn}-\text{Cu}_2\text{Mg}-\text{Mg}_2\text{Cu}$ eutectic [23]. Rapid quenching yielded an amorphous phase with traces of Mg_2Sn and Mg_2Cu .

The compositions of the following samples are located in regions of the ternary phase diagram for which no information about the equilibrium structure has hitherto been published. The crystalline phases reported were observed using XRD.

A8: $\text{Mg}_{61.20}\text{Cu}_{19.40}\text{Sn}_{19.40}$. The equilibrium phases observed were Cu_2Mg with 15 at % Sn in solid solution (in keeping with Pearson [24]), Mg_2Sn and a small quantity of Mg_2Cu . In the rapidly quenched samples, only the crystalline Mg_2Sn phase was detected.

A9: $\text{Mg}_{52}\text{Cu}_{24.10}\text{Sn}_{23.90}$. The crystalline phases observed were Cu_2Mg with 15 at % Sn in solid solution (cf. Pearson [24]), and Mg_2Sn . In addition, the X-ray diffractograms showed four unidentified lines. Rapid quenching afforded both crystalline phases, but the unidentified lines did not appear.

A10: $\text{Mg}_{33.3}\text{Cu}_{33.3}\text{Sn}_{33.3}$. The MgCuSn peak [25] and two unidentified peaks were observed. In the rapidly quenched samples, the ternary phase was also observed.

A11: $\text{Mg}_{16.66}\text{Cu}_{66.67}\text{Sn}_{16.66}$. Both the conventional alloy and the rapidly quenched samples consisted of crystalline Cu_4MgSn [25].

It should be mentioned that the results obtained by Sommer *et al.* [19] with a rotating wing device [26] do not contradict the results reported in this work, because their quenching rate (10^8 K s^{-1}) was faster than that attributed to the melt-spinning technique (10^6 K s^{-1}).

3. Theoretical model

For theoretical estimation of the composition region in which the alloy $\text{Mg}-\text{Cu}-\text{Sn}$ can form glasses when

rapidly quenched from the melt, we have used the model developed elsewhere [17], whose main ingredients are described below.

In the same way as for binary alloys [5–9], we write the enthalpy of formation of a ternary solid solution of metals A, B and C as

$$\Delta H_{\text{ABC}}^{\text{sol}} = \Delta H_{\text{ABC}}^{\text{c}} + \Delta H_{\text{ABC}}^{\text{e}} \quad (1)$$

where $\Delta H_{\text{ABC}}^{\text{c}}$ is a chemical contribution due to electron redistribution occurring when the alloy is formed, and $\Delta H_{\text{ABC}}^{\text{e}}$ is an elastic contribution due to atomic size mismatch. Strictly, a third contribution should perhaps be included in Equation 1 to take into account the possible differences in valence and crystal structure of the components. However, within the context of Miedema's model, this structural contribution can only be calculated for transition metal alloys in which the valence electrons occupy a common d-band, not for alloys which, like $\text{Mg}-\text{Cu}-\text{Sn}$, include non-transition metals; and in any case, neglect of the possible structural contribution should not substantially modify our results, because there are good reasons to believe that this contribution is considerably smaller than the other two [7].

As indicated elsewhere [17], the chemical contribution to the heat of formation of the ternary solid solution with atomic composition $(x_{\text{A}}, x_{\text{B}}, x_{\text{C}})$ can be calculated from the expression

$$\Delta H_{\text{ABC}}^{\text{c}} = \sum_{i < j} \frac{x_i x_j}{x'_i x'_j} \Delta H_{ij}^{\text{c}}(x'_i, x'_j) \quad (2)$$

where $\Delta H_{ij}^{\text{c}}(x'_i, x'_j)$ is the chemical contribution to the heat of formation of the associated binary alloy ij of composition (x'_i, x'_j) ($x'_i + x'_j = 1$) given by

$$x'_i = \frac{x_i}{x_i + x_j} \quad (3a)$$

$$x'_j = \frac{x_j}{x_i + x_j} \quad (3b)$$

The chemical contributions of the binary alloys can be computed, as indicated by De Boer *et al.* [11], in terms of the electronegativities, molar volumes and electron densities at Wigner-Seitz cell boundaries of the pure metals.

To calculate the elastic contribution to the heat of formation of ternary solid alloys, $\Delta H_{\text{ABC}}^{\text{e}}$, we have proposed a many-step process based on an extension of Eshelby's formula [10]. The original Eshelby formula is strictly valid for binary alloys at low solute concentration. The many-step method generalizes that used by López and Alonso [27] for binary alloys. For the reader's convenience, we briefly describe the basic ideas of this method for obtaining $\Delta H_{\text{ABC}}^{\text{e}}$ [17].

Consider the formation of a ternary alloy with n_i ($i = \text{A}, \text{B}, \text{C}$) moles of component i as a many-step process. Starting with n_{A} moles of the host metal A, we first add n_{B}^1 moles of metal B to form a dilute alloy ($n_{\text{B}}^1 \ll n_{\text{A}}$). Eshelby's elasticity theory affords the corresponding elastic energy as [10]

$$\Delta H^{\text{e}}(1) = x_{\text{B}}^1 \left[1 - x_{\text{B}}^1 \frac{(\gamma_1 - 1)\gamma_1}{(\beta_1 - 1)\beta_1} \right] \Delta h^{\text{e}}(\text{B in A}) \quad (4)$$

where Δh^e (B in A) is the elastic contribution to the heat of solution of B in A, given by

$$\Delta h^e(\text{B in A}) = \frac{2k_B\mu_A(V_A - V_B)^2}{3k_B V_A + 4\mu_A V_B} \quad (5)$$

$$\gamma_1 = 1 + \frac{4\mu_A}{3k_A} \quad (6)$$

and

$$\beta_1 = 1 + \frac{4\mu_A}{3k_B} \quad (7)$$

μ_A being the shear modulus of the host, k_A and k_B the bulk moduli of the host and solute metals, respectively, and V_A and V_B the atomic volumes. The composition x_B^1 is defined by

$$\begin{aligned} x_B^1 &= \frac{n_B^1}{n_A + n_B^1} \\ &\equiv \frac{1}{p} \left(\frac{n_B}{n_A + n_B} \right) \\ &= \frac{1}{p} \left(\frac{x_B}{x_A + x_B} \right) \end{aligned} \quad (8)$$

where p in the denominator indicates that the binary alloy A–B will be formed after p steps. The resulting dilute alloy is now considered as a monoatomic host A_1 with atomic volume

$$V_{A_1} = x_B^1 V_B + (1 - x_B^1) V_A \quad (9)$$

(from the Vegard law) and elastic constants

$$k_{A_1} = \frac{k_A k_B}{\alpha_1 k_A + (1 - \alpha_1) k_B} \quad (10)$$

and

$$\mu_{A_1} = \frac{\mu_A \mu_B}{\alpha_1 \mu_A + (1 - \alpha_1) \mu_B} \quad (11)$$

where α_1 is the volume concentration of B in the dilute alloy, given by

$$\alpha_1 = \frac{x_B^1 V_B}{x_B^1 V_B + (1 - x_B^1) V_A} \quad (12)$$

To this host A_1 a few more moles of component B, n_B^2 , are added, and the elastic energy is again calculated using Eshelby's equation as

$$\Delta H^e(2) = (x_B^2)^* \left\{ 1 - (x_B^2)^* \left[\frac{(\gamma_2 - 1)\gamma_2}{(\beta_2 - 1)\beta_2} \right] \right\} \Delta h^e(\text{B in } A_1) \quad (13)$$

where

$$\Delta h^e(\text{B in } A_1) = \frac{2k_B\mu_{A_1}(V_{A_1} - V_B)^2}{3k_B V_{A_1} + 4\mu_{A_1} V_B} \quad (14)$$

$$\gamma_2 = 1 + \frac{4\mu_{A_1}}{3k_{A_1}} \quad (15)$$

and

$$\beta_2 = 1 + \frac{4\mu_{A_1}}{3k_B} \quad (16)$$

In Equation 13, $(x_B^2)^*$ is a fictitious B-composition given by

$$(x_B^2)^* = \frac{n_B^2}{n_A + n_B^1 + n_B^2} \quad (17)$$

and is to be distinguished from the net B-composition at this stage of the process, given by

$$\begin{aligned} x_B^2 &= \frac{n_B^1 + n_B^2}{n_A + n_B^1 + n_B^2} \equiv 2x_B^1 \\ &= \frac{2}{p} \left(\frac{x_B}{x_A + x_B} \right) \end{aligned} \quad (18)$$

The process can be continued in this way to form, after a sufficient number of steps, p , the binary alloy A–B. It is now this binary alloy that is considered as a host to which a few moles of component C, n_C^1 , are added; this allows Eshelby's equation to be used once more to calculate the elastic energy. The process can then be repeated a sufficient number of steps, q , until finally the ternary alloy A–B–C with the desired composition (x_A, x_B, x_C) is obtained. The total elastic energy of the alloy (per mole of the final ternary alloy) is calculated by adding the elastic energies corresponding to every step

$$\begin{aligned} \Delta H_{ABC}^e &= \sum_{m=1}^{p-1} \Delta H^e(m) P(m) \\ &\quad + \Delta H^e(p)(x_A + x_B) \\ &\quad + \sum_{n=1}^{q-1} \Delta H^e(p+n) Q(n) \\ &\quad + \Delta H^e(p+q) \end{aligned} \quad (19)$$

where the factors $P(m)$ and $Q(n)$ are given by

$$P(m) = \left(\prod_{k=m+1}^p [1 - (x_B^k)^*] \right) \left(\left[\prod_{l=1}^q [1 - (x_C^l)^*] \right] \right) \quad (20)$$

$$Q(n) = \prod_{k=n+1}^q [1 - (x_C^k)^*] \quad (21)$$

In the amorphous state the elastic contribution is absent (or at least is much smaller than in the solid solution), so that the enthalpy of formation can be written as

$$\begin{aligned} \Delta H_{ABC}^{am} &= \Delta H_{ABC}^c + x_A \Delta H_A^{a-s} \\ &\quad + x_B \Delta H_B^{a-s} + x_C \Delta H_C^{a-s} \end{aligned} \quad (22)$$

where ΔH_i^{a-s} is the enthalpy difference between the amorphous and crystalline states of pure element i . To compute these quantities we have used the equation proposed by Van Der Kolk *et al.* [6].

$$\Delta H_i^{a-s} = \alpha T_{m,i} \quad (23)$$

where $\alpha = 3.5 \text{ J mol}^{-1} \text{ K}^{-1}$ and $T_{m,i}$ is the melting temperature of component i . In Equation 22, the chemical contribution ΔH_{ABC}^c , given by Equation 2, has been obtained taking into account the occurrence of chemical short-range order in amorphous alloys [28]. We have also assumed that the solid solution has the same degree of short-range order as the amorphous alloy.

To compute the Gibbs free energies of the various phases, which show their relative stabilities, the entropies of mixing have also to be specified. In our calculations we have, for simplicity, assumed the ideal solution model for the entropy of mixing in both the amorphous and solid solution phases, i.e.

$$\Delta S = -R(x_A \ln x_A + x_B \ln x_B + x_C \ln x_C) \quad (24)$$

where R is the gas constant. However, it should be borne in mind that the configurational entropy is very much the same in these two phases [29], so that a more realistic approximation for the entropy of mixing will simply shift the corresponding Gibbs free energy surfaces without changing their relative positions.

4. Glass formation in Mg–Cu–Sn

In Fig. 1 we show the glass-forming diagram calculated for the system Mg–Cu–Sn. The calculations

were carried out for room temperature, at which the values of the elastic coefficients of the pure metals (needed for obtaining ΔH_{ABC}°) are available [30]. Several regions can be distinguished in the diagram. In the region labelled A the free energy of the amorphous phase is more negative than that of the solid solution and the system should, in principle, be readily amorphized. In the region labelled S, the solid solution is more stable than the amorphous phase. In the regions labelled I, the system is unstable and consists of a simple mixture of the unreacted crystalline elements. The amorphous region is bounded by what are called T_0 curves [1, 31], which are defined by the compositions at which the free energies of the amorphous phase and the solid solution have the same value.

Fig. 1 shows the compositions of the samples A_4, A_5, A_6, B_3 and B_5 of section 2 which afforded homogeneous amorphous Mg–Cu–Sn alloys under single-roller melt-spinning at an estimated cooling rate of 10^6 K s^{-1} , the compositions of the partially

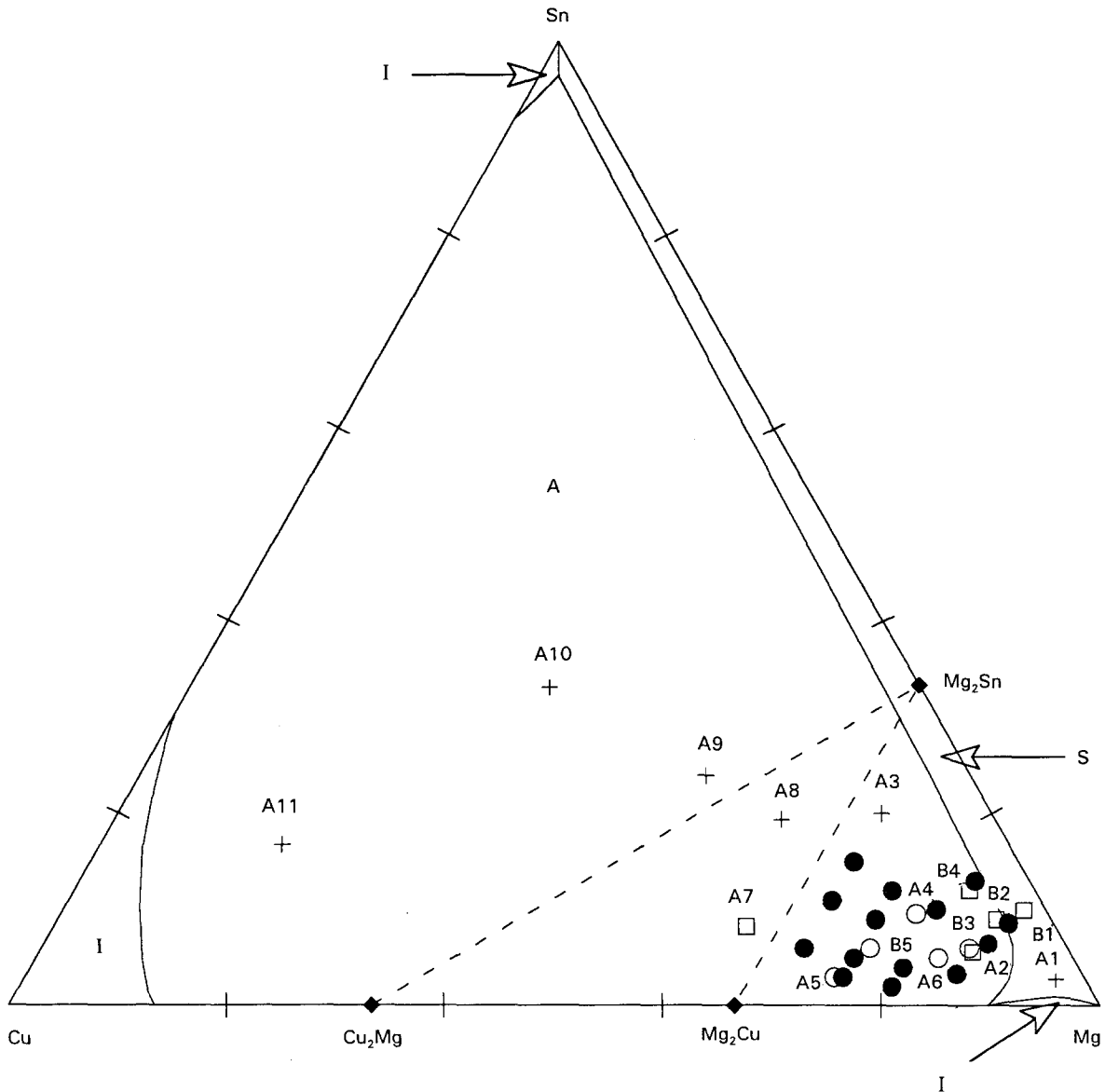


Figure 1 Glass-forming diagram for the ternary Mg–Cu–Sn system calculated by considering competition between amorphous (A) and solid solution (S) phases. The permissible region for the latter is delimited by the T_0 (—) curves. In regions labelled I the system consists of a mixture of the unreacted crystalline elements. Rapidly quenched samples A1–A11 and B1–B5, discussed in Section 2: (O) totally amorphous, (□) partially amorphous, (x) crystalline. (●) The compositions at which Sommer *et al.* [19] found homogeneous amorphous phases (---) lines joining the intermetallic compounds Mg_2Sn , Cu_2Mg and Mg_2Cu .

amorphized samples A₂, A₇, B₁, B₂ and B₄; and the compositions for which only crystalline phases were identified (samples A₁, A₃, A₈, A₉, A₁₀ and A₁₁). The compositions at which Sommer *et al.* [19] achieved total amorphization using a rotating wing apparatus, which allows cooling rates as fast as 10⁸ K s⁻¹ are also shown. All the compositions for which amorphous phases have been identified are located in the magnesium-rich corner of the diagram, and all are included in the predicted glass-forming region A, except one point (B₁) which is just outside the boundary of A. Some of the points of partial amorphization (A₂, B₂ and B₄) are close to compositions at which Sommer *et al.* [19] achieved a homogeneous amorphous phase, this difference in behaviour probably being due to the different cooling rates attained in their work and ours.

In connection with the latter result, it should be pointed out that the theoretical amorphization diagram of Fig. 1 assumes that the formation of energetically more stable intermetallic compounds can be inhibited kinetically. As indicated elsewhere [17], the possible interference of these compounds must be taken into account to explain the differences between the results obtained in a given experiment and the glass-forming composition range predicted by comparing only the free energies of the amorphous phase and the solid solution. In the case of the binary alloy Mg–Cu, this point has been discussed in detail by de Tandler *et al.* [9], who showed how the role played by the intermetallic compound Cu₂Mg must be taken into account in interpreting the experimental range of total amorphization of Mg–Cu reported by Sommer *et al.* [32]. Cu₂Mg has a simple fcc crystal structure, so that the process of nucleation and growth of the compound competes with the formation of the amorphous phase.

For the ternary alloy that we are now considering, it may firstly be pointed out that tin and magnesium have a strong tendency to association, not only in the melt [33] but also in the undercooled or amorphous state [34]. In rapidly quenched samples, this gives rise to the presence, in the amorphous material, of clusters of stoichiometric Mg₂Sn, which at certain alloy compositions can segregate to form a crystalline Mg₂Sn phase if cooling is not fast enough to ensure completely amorphous samples. This explains the partial amorphization of melt-spun samples with compositions B₂ and B₄, which were a mixture of the amorphous phase and the compound Mg₂Sn together with magnesium crystals (whereas at similar compositions, complete amorphization, in keeping with the predicted amorphization region, was achieved by Sommer *et al.* [19] using a faster cooling rate).

The points labelled A₁₀ and A₁₁ in Fig. 1 correspond to the compositions of the intermetallic compounds MgCuSn and Cu₄MgSn, respectively. Their calculated free energies are respectively –11.8 and –10.6 kJ mol⁻¹, while the free energies of the amorphous phase at these compositions are –8.7 and –6.6 kJ mol⁻¹. Because the compounds have simple fcc crystal structures [21], they can compete well with the amorphization process, which explains their appearance in the rapid-quenching experiments.

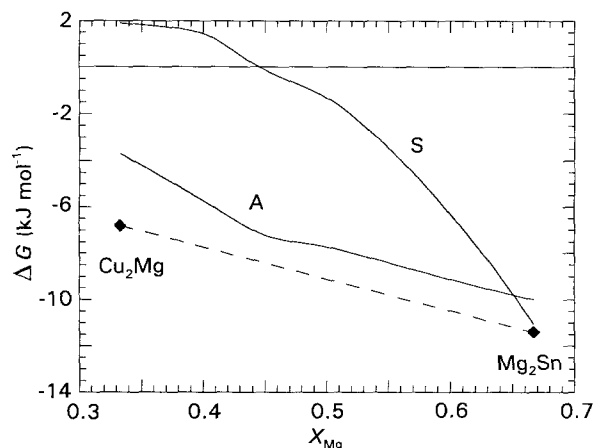


Figure 2 Calculated free energies of the solid solution (S) and the amorphous phase (A) along the straight line joining the intermetallic compounds Cu₂Mg and Mg₂Sn. The free energies of these compounds, calculated as indicated elsewhere [7, 11], are also shown in the figure.

The rapid-quenching results corresponding to other points of Fig. 1 are likewise impossible to explain solely in terms of competition between the amorphous and solid solution. The alloy composition labelled A₉, for instance, is near the straight line between the points corresponding to the binary compounds Mg₂Sn and Cu₂Mg. The free energy of a mechanical mixture of these two compounds is lower than that of the competing ternary amorphous alloy (Fig. 2), so that these compounds must appear in the quenched samples unless they are by-passed kinetically, which does not occur (Table I). A similar interpretation can be given to the rapid-quenching result corresponding to the point A₃ of Fig. 1, which is close to the straight line between the points corresponding to the binary compounds Mg₂Cu and Mg₂Sn. Of course, a more quantitative interpretation of the rapid-quenching results of Fig. 1, including those for samples in which the amorphous alloy coexists with crystalline phases, would require the construction of the metastable equilibrium phase diagram using the common-tangent-plane method [35]. However, this is a non-trivial task which requires very accurate estimation of the free energies of the phases involved, and it has not been attempted in this work. Additionally, it is not clear to what extent metastable equilibrium actually occurs in real samples.

Some considerations are in order with respect to the binary systems Mg–Cu, Cu–Sn and Mg–Sn associated with the ternary alloy Mg–Cu–Sn. As indicated above, the binary system Mg–Cu has been studied in detail by de Tandler *et al.* [9] who, like us, used Miedema's theory, but in a way differing in some respects from our approach here. Specifically, de Tandler *et al.*'s calculations were carried out assuming that both the amorphous phase and the solution are statistically ordered, whereas we have performed more realistic calculations considering the presence of chemical short-range order [28]; moreover, de Tandler *et al.* obtained free energies for 380 K (the glass temperature of Mg–Cu at the eutectic composition $x_{Cu} = 0.145$ [32]), whereas our calculations have been carried out

for room temperature, for which the elastic coefficients of the pure metals are known [30]. In spite of these differences, it is worth noting that, according to Fig. 1, the glass-forming region for Mg–Cu would, if the formation of intermetallic compounds could be kinetically inhibited, be $0.13 \leq x_{\text{Mg}} \leq 0.90$, which is very close to the range $0.12 \leq x_{\text{Mg}} \leq 0.92$ found by de Tandler *et al.* Similarly, the glass-forming range for Cu–Sn in Fig. 1, $0.08 \leq x_{\text{Cu}} \leq 0.70$, is in reasonable agreement with the experimental result $0.1 \leq x_{\text{Cu}} \leq 0.8$ obtained by Korn *et al.* [36, 37] using flash evaporation and deposition on cold substrate, which achieves high quenching rates and so prevents the formation of any crystalline phases. Finally, our prediction that Mg–Sn is not a good glass former (Fig. 1 shows the solid solution to be more stable than the amorphous phase over the whole range of concentrations) is also in agreement with experiment [14]; as noted above, the amorphization of this system is made even more unlikely by the strong tendency of magnesium and tin to associate, which readily gives rise to the formation of nuclei for the crystallization of Mg_2Sn .

5. Conclusion

The model used in this work, which is basically an extension of Miedema's theory to ternary alloys, predicts an extensive glass-formation region for the system Mg–Cu–Sn. Our predictions are in agreement with our experimental results on magnesium-rich Mg–Cu–Sn glasses and with available information for the associated binary alloys. The discrepancies between the concentration region obtained by comparing the free energies of the amorphous phase and the solid solution and the results of certain experiments can be explained in terms of the influence of competing crystalline compounds.

Acknowledgements

This work was supported by the DGICYT, Spain (Project nos PB89-0352-C02 and PB92-0645-C03), the Xunta de Galicia (Project no. XUGA20602B92), the Spanish Ministry of Education and Science's Programme for Scientific Cooperation with Hispano-América, and CONICET and UBA (Argentina).

References

1. W. L. JOHNSON, *Prog. Mater. Sci.* **30** (1986) 81.
2. J. JÄCKLE, *Rep. Prog. Phys.* **49** (1986) 171.
3. K. SAMWER, *Phys. Rep.* **161** (1988) 1.
4. F. SOMMER, in "Proceedings of the Fifth International Conference on Rapidly Quenched Metals", edited by S. Steeb and H. Warlimont (North-Holland, Amsterdam, 1985), p. 153.
5. P. I. LOEFF, A. W. WEEBER and A. R. MIEDEMA, *J. Less-Common Metals* **140** (1988) 299.
6. G. J. VAN DER KOLK, A. R. MIEDEMA and A. K. NIESSEN, *ibid.* **145** (1988) 1.

7. J. M. LOPEZ, J. A. ALONSO and L. J. GALLEG0, *Phys. Rev.* **B36** (1987) 3716.
8. L. J. GALLEG0, J. A. SOMOZA, H. M. FERNANDEZ and J. A. ALONSO, *J. Phys. Coll. C4* **51** (1990) 111.
9. R. H. DE TENDLER, J. A. KOVACS and J. A. ALONSO, *J. Mater. Sci.* **27** (1992) 4935.
10. J. D. ESHELBY, *Solid State Phys.* **3** (1956) 79.
11. F. R. DE BOER, R. BOOM, W. C. M. MATTENS, A. R. MIEDEMA and A. K. NIESSEN, "Cohesion in Metals" (North-Holland, Amsterdam, 1988).
12. N. SAUNDERS and A. P. MIODOWNIK, *J. Mater. Res.* **1** (1986) 38.
13. R. BORMANN, F. GÄRTNER and K. ZÖLTZER, *J. Less-Common Metals* **145** (1988) 19.
14. F. SOMMER, M. FRIPAN and B. PREDEL, in "Proceedings of the Fourth International Conference on Rapidly Quenched Metals", Vol. 1, edited by T. Masumoto and K. Suzuki (Japan Institute of Metals, Tokyo, 1982), p. 209.
15. S. UENO and Y. WASEDA, *Sci. Rep. Res. Inst. Tohoku Univ. A* **32** (1985) 97.
16. T. EGAMI and Y. WASEDA, *J. Non-Crystalline Solids* **64** (1984) 113.
17. J. A. SOMOZA, L. J. GALLEG0, C. REY, H. M. FERNANDEZ and J. A. ALONSO, *Philos. Mag.* **B65** (1992) 989.
18. C. G. WOYCHIK and T. B. MASSALSKI, in "Proceedings of the Fifth International Conference on Rapidly Quenched Metals", edited by S. Steeb and H. Warlimont (North-Holland, Amsterdam, 1985) p. 207.
19. F. SOMMER, H. HAAS and B. PREDEL, in "Phase Transformation in Crystalline and Amorphous Alloys", edited by B. L. Mordike (DGM, Oberursel, 1983) p. 95.
20. H. SIRKIN, N. MINGOLO, E. NASSIF and B. ARCONDO, *J. Non-Crystalline Solids* **93** (1987) 323.
21. Y. A. CHANG, J. P. NEUMANN, A. MIKULA and D. GOLDBERG, in "Phase Diagrams and Thermodynamic Properties of Ternary Copper-Metal Systems", INCRA Monograph VI, USA (1979) p. 520.
22. E. E. VICENTE, S. BERMUDEZ, A. ESTEBAN, R. DE TENDLER, B. ARCONDO and H. SIRKIN, *J. Mater. Sci.* **26** (1991) 1327.
23. E. E. VICENTE, personal communication (1993).
24. W. B. PEARSON, "Handbook of Lattice Spacings and Structures of Metals and Alloys", Vol. 2 (Pergamon Press, New York, 1967).
25. K. OSAMURA and Y. MURAKAMI, *J. Less-Common Metals* **60** (1978) 311.
26. G. DUDDEK and B. PREDEL, *Z. Metallkde* **69** (1978) 773.
27. J. M. LÓPEZ and J. A. ALONSO, *Phys. Status Solidi A* **85** (1984) 423.
28. A. W. WEEBER, *J. Phys. F* **17** (1987) 809.
29. A. R. MIEDEMA and A. K. NIESSEN, *Suppl. Trans. Jpn Inst. Metals* **29** (1988) 209.
30. K. A. GSCHNEIDNER Jr, *Solid State Phys.* **16** (1964) 275.
31. T. B. MASSALSKI, in "Proceedings of the Fourth International Conference on Rapidly Quenched Metals", edited by M. Masumoto and K. Suzuki (Japan Institute of Metals, Tokyo, 1982) p. 203.
32. F. SOMMER, G. BUCHER and B. PREDEL, *J. Phys. Coll. C8* **41** (1980) 563.
33. S. STEEB and H. ENTRESS, *Z. Metallkde* **57** (1966) 803.
34. B. JÖNSSON and J. AGREN, *Met. Trans.* **17A** (1986) 607.
35. L. KAUFMAN and H. BERNSTEIN, "Computer Calculation of Phase Diagrams" (Academic Press, New York, 1970).
36. D. KORN, W. MÜRER and G. ZIBOLD, *Z. Phys.* **260** (1973) 351.
37. D. KORN, W. MÜRER and G. ZIBOLD, *J. Phys. Coll. C4* **35** (1974) 257.

Received 15 February
and accepted 9 June 1994